A First-Principles Study: Structure and Decomposition of Mono-/Bimetallic Ammine Borohydrides

ARTICLE *in* THE JOURNAL OF PHYSICAL CHEMISTRY C · APRIL 2014

Impact Factor: 4.77 · DOI: 10.1021/jp5012439

5 AUTHORS, INCLUDING:

Kun Wang
Beijing Institute of Technology
34 PUBLICATIONS **72** CITATIONS

SEE PROFILE

Jian-Guo Zhang
Beijing Institute of Technology
303 PUBLICATIONS **1,528** CITATIONS

SEE PROFILE

THE JOURNAL OF PHYSICAL CHEMISTRY C

Article

pubs.acs.org/JPCC

A First-Principles Study: Structure and Decomposition of Mono-/Bimetallic Ammine Borohydrides

Kun Wang,[†,‡] Jian-Guo Zhang,*[,†] Jian-She Jiao,[§] Tonglai Zhang,[†] and Zun-Ning Zhou[†]

[†]State Key Laboratory of Explosion Science and Technology, Beijing Institute of Technology, Beijing 100081, People's Republic of China

[‡]Department of Chemistry, Inorganic Chemistry Laboratory, University of Oxford, South Parks Road, Oxford OX1 3QR, United Kingdom

[§]General Armament Department, Research Institute of FA and ADA Equipment and Technology, Beijing 100012, People's Republic of China

ABSTRACT: Bimetallic ammine borohydrides have been demonstrated to be capable of improving the efficiency of dehydrogenation and purity of the released hydrogen as compared to monometallic AMBs. We have obtained the optimized structures, orbital, and decomposition thermodynamic properties of several metal ammine borohydrides (AMB) containing $[Li(BH_4)_n]^{1-n}$ groups by performing a solid-state density functional theory calculation. The structures are abbreviated as $M-Li(BH_4)_x(NH_3)_y$, where M means Li, Mg, Al, and Ca, respectively. $[LiBH_4]$ segments in these compounds play a crucial role in suppressing borane emission. Additionally, it activates the B−H···H−N bonds and decreases the hydrogen removal energies. Furthermore, the strength of M−N bonds will dictate the impurity of the ammine from the decomposition. The stability of the AMBs can be found as follows from the results of orbitals: $LiMg(BH_4)_3(NH_3)_2$ > $Li_2Al(BH_4)_5(NH_3)_4$ > $LiCa(BH_4)_3(NH_3)_2$ > $[Li(BH_4)(NH_3)]_2$. Finally, the $[LiBH_4]$ group can polarize the molecule and improve the efficiency of dehydrogenation process and purity of released hydrogen from bimetallic ammine borohydrides (AMBs) as compared to monometallic AMBs, which is due to the different bond strengths of M−B and M−N bonds (M denotes different metal cations here).

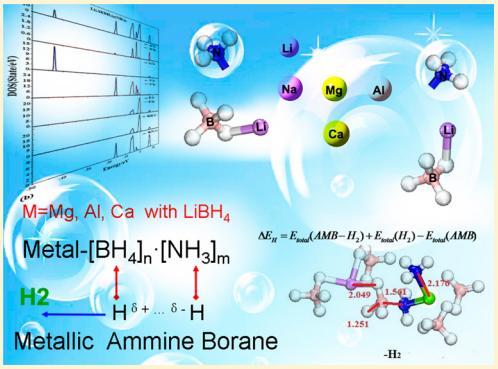

1. INTRODUCTION

Hydrogen is a promising alternative energy carrier because it is the most abundant and clean resource and it has a high energy content. However, hydrogen storage is one of the key challenges in developing it as a fuel for vehicles.[1−8] Metallic ammine borohydrides (AMB) have recently emerged as attractive candidates for hydrogen storage materials because of their high percentage of available hydrogen.[9−14] It was demonstrated that upon forming ammoniates, hydrogen can be more readily produced through the local interaction of the protic hydrogen atoms in NH_3 and the hydridic hydrogen atom in $[BH_4]^-$ groups without necessarily involving an interfacial reaction or mass transport through different phases for the amide−hydride connections.[9,15,16] A variety of novel, promising AMB materials have been designed and synthesized. The off-board regeneration has been attempted for some of these materials.[17] Some excellent monometallic AMBs, such as $Mg(BH_4)_2{\cdot}2NH_3$,[9] $Ti(BH_4)_3{\cdot}3NH_3$,[13] and $Zn(BH_4)_2{\cdot}2NH_3$,[10] can release nearly pure hydrogen without any catalysts. However, some monometallic AMBs exhibited weak dehydrogenation properties, such as $Li(BH_4){\cdot}NH_3$, $Y(BH_4)_3{\cdot}3NH_3$, and $Al(BH_4)_3{\cdot}2NH_3$. That is because the dehydrogenation properties are strongly affected by not only the metal cations, but also the coordination number of ammonia. This effect, however, changes immensely if the monometallic AMBs interact with the metal tetrahydroborates, such as $LiBH_4$, $NaBH_4$, or $Mg(BH_4)_2$.[18−20]

Materials composed of different metal cations have been previously reported to improve dehydrogenation properties.[21−23] A lot of research has focused on $LiBH_4$ because it possesses an extremely high hydrogen content (18.4 wt %). It is a notable compound for its ability to improve the purity of hydrogen in the product and decrease dehydrogenation temperatures when mixing with some monometallic AMBs, which have been experimentally demonstrated,[24] such as $Ti(BH_4)_3{\cdot}5NH_3$ and $Li_2Ti(BH_4)_5{\cdot}5NH_3$.[13] $Ti(BH_4)_3{\cdot}5NH_3$ releases a lot of ammonia in its decomposition, whereas for the compound of $Li_2Ti(BH_4)_5{\cdot}5NH_3$, hydrogen is almost the only product in the temperature range of 75−300 °C.[13] A similar phenomenon can be seen between $Al(BH_4)_3{\cdot}5NH_3$ and $LiAl(BH_4)_4{\cdot}4NH_3$ and $Ca(BH_4)_2{\cdot}NH_3$ and $LiCa(BH_4)_3{\cdot}NH_3$.[15,25,26] What is more, for those monometallic AMBs (such as $Mg(BH_4)_2{\cdot}2NH_3$ and $Zn(BH_4)_2{\cdot}2NH_3$) that can release high-purity hydrogen with one metal ion, the decomposition temperature will be extremely decreased when

Received: February 4, 2014
Published: March 28, 2014

   dx.doi.org/10.1021/jp5012439 | J. Phys. Chem. C 2014, 118, 8271−8279

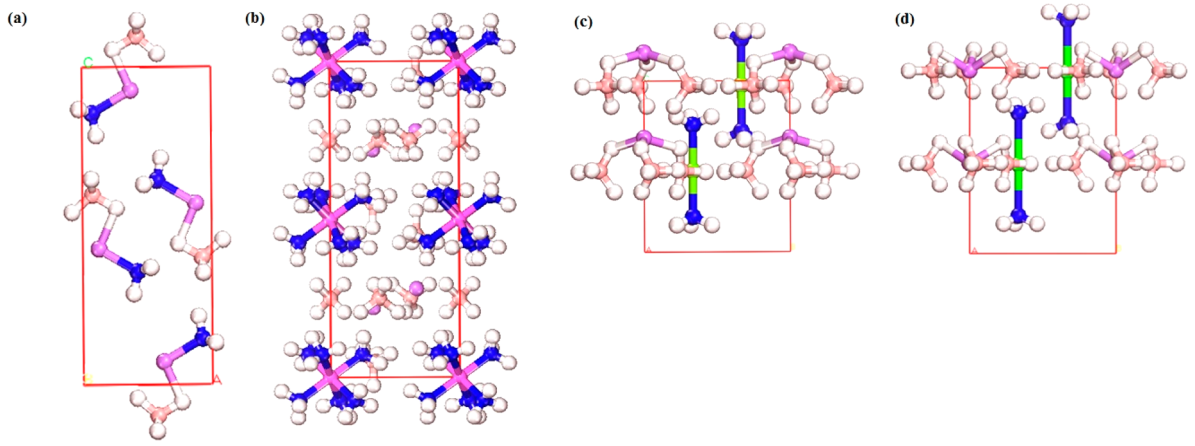

Figure 1. Crystal structures of the title compounds: (a) $[Li(BH_4)(NH_3)]_2$ (viewing direction: [100]), (b) $Li_2Al(BH_4)_5(NH_3)_6$ (viewing direction: [100]), (c) $LiMg(BH_4)_3(NH_3)_2$ (viewing direction: [001]), and (d) $LiCa(BH_4)_3(NH_3)_2$ (viewing direction: [001]). The blue, light pink, light purple, and white represent N, B, Li, and H. Dark purple in (b) denotes Al, green in (c) denotes Ca, while green means Mg in (d).

Table 1. Comparison between Calculated and Experimental Cell Parameters and Bond Lengths (Å) of the Four Title Compounds

	ALLB		AALB		AMLB		ACLB	
	theor	exp	theor	exp	theor	exp	theor	exp[a] [25]
a (Å)	5.90	5.96	7.68	7.79	7.91	8.00	8.23	
b (Å)	4.48	4.46	7.68	7.79	7.91	8.00	8.23	
c (Å)	14.52	14.34	16.31	15.96	8.02	8.42	9.02	
α (deg)	90	90	90	90	90	90	90	
β (deg)	90	90	90	90	90	90	90	
γ (deg)	90	90	120.00	120.00	120.00	120.00	9.02	
Li−B	2.48	2.52−2.57	2.45−2.78	2.52−2.58	2.72	2.31−2.51	2.29	
N−H	1.03	1.17	1.04	1.03	1.03	1.05	1.03	
B−H	1.22	0.95	1.23	1.23	1.22−1.23	1.23−1.25	1.23	
M−N[b]	2.04	2.01	2.05	1.62−2.01	2.15	2.04−2.20	2.49−2.50	
M−B	2.48	2.52	4.80	5.00	2.57	2.58	2.77	2.95
NH−HB	2.20−2.44	2.55	1.93−2.04	2.02−2.26	2.23	2.19−2.27	2.37	2.09

[a]The experimental value is from $Ca(BH_4)_2(NH_3)$. [b]M = Li, Al, Mg, Ca.

mixing $LiBH_4$, as is the case with $LiZn(BH_4)_3{\cdot}4NH_3$[10] and $LiMg(BH_4)_3{\cdot}2NH_3$[27] as compared to $Zn(BH_4)_2{\cdot}2NH_3$[10] and $Mg(BH_4)_2{\cdot}2NH_3$,[9] respectively.

To understand the mechanism of bimetallic ammine borohydrides containing a $[LiBH_4]$ group, we employed first-principles calculations to investigate the optimized crystal structures, electronic structures, and thermodynamic properties of the decomposition, including the energies of dehydrogenation, deammoniation, and removal of borane in solid $Li_2Al(BH_4)_5(NH_3)_6$ (AALB), $LiMg(BH_4)_3(NH_3)_2$ (AMLB), $LiCa(BH_4)_3(NH_3)_2$ (ACLB), and $[Li(BH_4)(NH_3)]_2$ (ALLB). ALLB here is a monometallic AMB and designed for the comparison with other bimetallic AMBs. To date, the crystal structures of $LiMg(BH_4)_3(NH_3)_2$,[27] $Li_2Al(BH_4)_5(NH_3)_6$,[28] and $Li(BH_4)(NH_3)$[29] have been experimentally determined. We also design the structure of ACLB by substituting Mg^{2+} in AMLB with Ca^{2+}. Generally, AMBs or amidoborane compounds with the metal cations sharing the same elemental group are isostructural, for example, $Mg(BH_4)_2{\cdot}2NH_3$ and $Ca(BH_4)_2{\cdot}2NH_3$[9,15] and KNH_2BH_3, $LiNH_2BH_3$, and $NaNH_2BH_3$;[30−32] therefore, it is reasonable to expect that $LiCa(BH_4)_3(NH_3)_2$ and $LiMg(BH_4)_3(NH_3)_2$ are also isostructural.

2. COMPUTATIONAL METHODS

First-principles calculations were carried out within the DFT calculations using the projector augmented wave (PAW) method,[33] which is implemented in the CASTEP package.[34] The generalized gradient approximation[35] of Perdew, Burke, and Ernzerhof[36] (GGA-PBE) for the exchange-correlation function has been used throughout the CASTEP calculations. The Vanderbilt-type ultrasoft pseudopotentials[37] with valence states $2p^63s^2$ for Mg, $3s^23p^64s^2$ for Ca, $3s^23p^1$ for Al, $1s^22s^1$ for Li, $2s^22p^1$ for B, $2s^22p^3$ for N, and $1s^1$ for H were used to describe the core electrons. A plane wave basis set with an energy cutoff of 500 eV was used. The Brillouin zone integration of ALLB, AALB, AMLB, and ACLB were performed by using 2 × 2 × 2, 4 × 4 × 3, 4 × 4 × 3, and 5 × 6 × 2 Monkhorst Pack meshes,[38] respectively. Structural relaxations of atomic positions, cell parameters, and volume during geometry optimization were carried out by the Broyden−Fletcher−Goldfarb−Shanno (BFGS) method[39] until the residual forces and stresses were less than 0.005 eV/Å and 0.05 GPa.

3. RESULTS AND DISCUSSION

3.1. Structure. Figure 1 shows the cell structures of ALLB, AALB, AMLB, and ACLB. The cell parameters and selected

dx.doi.org/10.1021/jp5012439 | J. Phys. Chem. C 2014, 118, 8271−8279

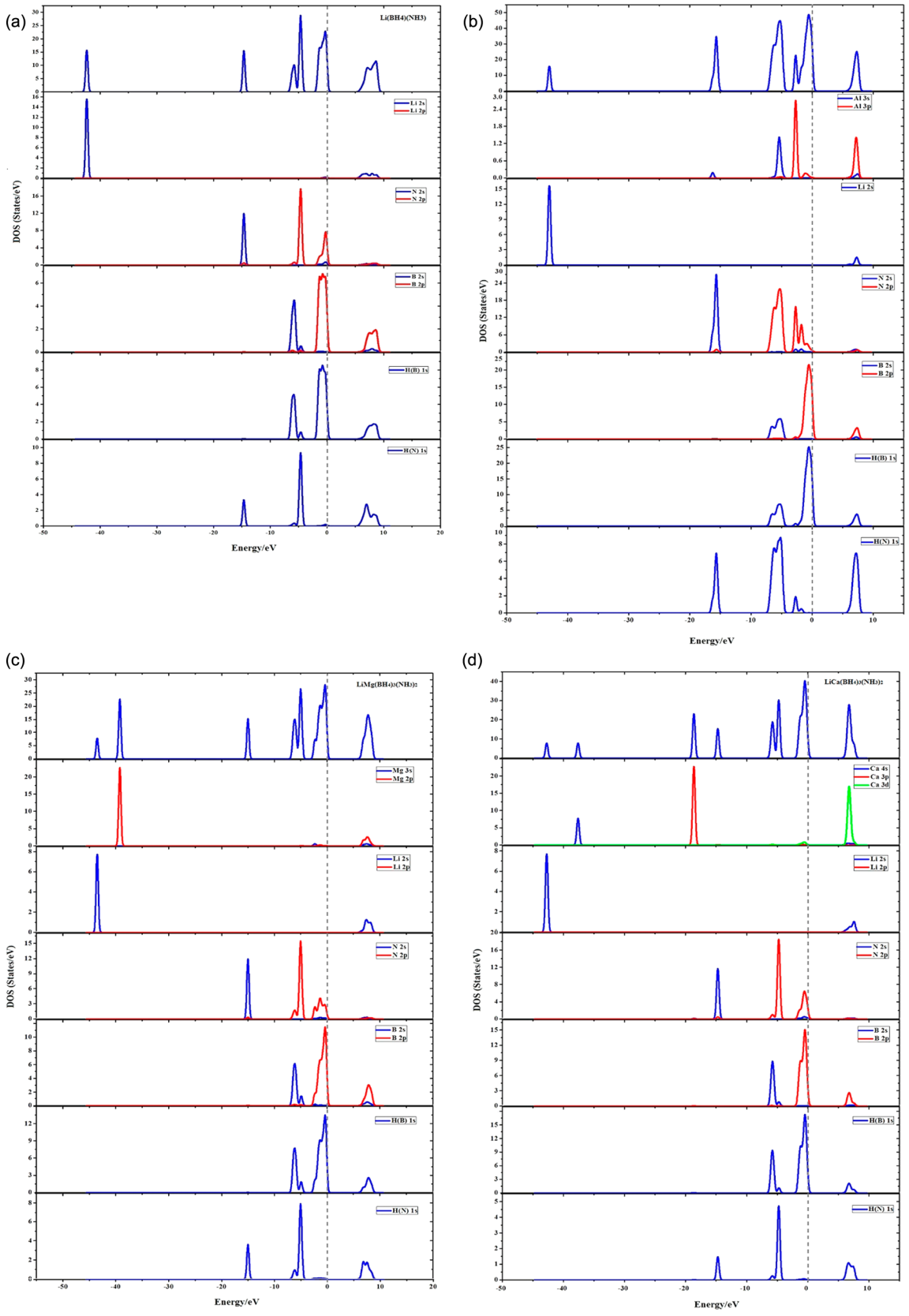

Figure 2. Total and partial electronic DOSs of (a) ALLB, (b) AALB, (c) AMLB, and (d) ACLB. The s-electron contributions are depicted with a blue solid line, and the p-states are depicted with a red solid line. The Fermi level is set as zero energy.

bond lengths of each structure were summarized and compared to the available experimental results (except for ACLB) in Table 1. In general, the calculated results are in agreement with the available experiment data. The crystal ALLB adopts orthorhombic symmetry in space group *Pnma*. In crystalline ALLB, each Li^+ is coordinated to one $[BH_4]^-$ group through

dx.doi.org/10.1021/jp5012439 | J. Phys. Chem. C 2014, 118, 8271−8279

H^+ and one $[NH_3]$ group through N, with a bond angle ∠N−Li−H(B) of 97.70°. Li, N, and B atoms are almost aligned in the same [100] plane. The crystal AALB adopts trigonal space group *P*3*c*1. The Al cations in crystalline AALB coordinate octahedrally to six $[NH_3]$ groups symmetrically (∠N−Al−N = 90.00°), while Li cations coordinate to four $[BH_4]$ anions forming a tetrahedral structure (∠B−Li−B = 116.07°). Each tetrahedral $[Li(BH_4)_4]^{3-}$ is bridged by H atoms spread along a plane perpendicular to the [100] plane. Both AMLB and ACLB having similar structures in our calculation adopt hexagonal symmetry in space group *P*63. In both structures, the Mg^{2+} (or Ca^{2+}) cation coordinates to two aligned $[NH_3]$ molecules linearly where the bonds of N−Mg−N/N−Ca−N are parallel to the *c*-axis, while the Li cation coordinates to three $[BH_4]$ anions with the following bond angles: ∠H(B)−Li−H(B) is 113.70° in AMLB and 98.53° in ACLB. The direction of the bridging groups of $[BH_4]$ anions is perpendicular to the [001] plane.

3.2. Electronic Structures and Bonding Character. The total and partial densities of state (DOS) of the four AMBs are shown in Figure 2 to illustrate the relationship between the electronic structure and the bonding characteristics. The calculated band gap of ALLB is 5.72 eV, which might be underestimated as is typical of GGA calculations for the band gap;[40,41] nonetheless, it strongly indicates that ALLB is a wide band gap insulator. Figure 2a shows the calculated total and partial DOS for solid ALLB. It can be seen that the total DOS of ALLB is composed of five groups. The lowest-energy region is dominated by Li 2s states from −45 to −40 eV. The next group at about −20 to −10 eV mainly consists of the N 2s states and has a small contribution from H(N) 1s states. The third region, around −10 to −4 eV, is filled by N 2p and B 2s states hybridized with H 1s states. The top of the valence band consists of B 2p and H(B) 1s states. The distribution of Li 2s states in the valence band shows the strong ionic interaction between Li and B.

Our calculated DFT electronic band gap of AALB is approximately 6.09 eV, indicating AALB is also a wide band gap insulator. As seen in Figure 2b, the valence band is well separated into three regions. The top of the valence band consists of several peaks coming from Al 3s, Al 3p, N 2p, B 2p, and H 1s states along with a very small participation by the N 2s states. It reveals the covalent nature of the Al−N bonds. The Li 2s states constitute the lowest region of the valence band. The third region, about −20 to −10 eV, is mainly composed of N 2p and H(N) 1s states with a small contribution by Al 3s states. The distribution of Li 2s states corroborates the ionic nature of the interaction between Li and B. Thus, we can conclude that the relationship between Li−BH_4 sections in the compound is of an ionic nature, while the distribution of Al 3s, Al 3p, and N 2p states indicates some covalent character of Al−N bonds.

As for AMLB and ACLB, both exhibit nonmetallic features with finite energy gaps between valence bands and conduction bands. The calculated GGA band gaps of AMLB and ACLB are approximately 6.45 and 6.13 eV, respectively. Figure 2c and d shows the calculated total and partial DOS values of AMLB and ACLB. They exhibited similar distribution, and they have four groups in the valence band. The lowest regions of them are dominated by Li 2s states from −45 to −40 eV. The tops of the valence bands are both composed of N 2s, B 2s, B 2p, and H 1s states. The only notable difference between them is that some covalent characteristic appears between the Ca and N atoms in the energy range of −20 to −10 eV. Generally, the strong sp hybridization of states between N, B, and H atoms in all three MABs suggests a covalent nature of B−N, N−H, and B−H bonds. It seems that two metal cations play two different roles in bimetallic AMBs: Li^+ will bond to the $[BH_4]$ group by the strong electrostatic potential; while the other metal (Mg/Al/Ca) cation will interact with ammonia with both ionic or covalence bonds.

3.3. Population and Reactivity. Before further discussing the possible decomposition of the four compounds, we present compared results of the calculated population of the selected chemical bonds to obtain the strength between different bonds. The HOMO−LUMO energy gap has been simultaneously calculated in each case to show the stability. The results have been listed in Table 2.

Table 2. Population of the Selected Bonds in the Dissociation and Their HOMO−LUMO Energy Gap

	ALLB	AALB	AMLB	ACLB
B−H	0.98	0.96	0.98	0.97
N−H	0.71	0.73	0.76	0.69
M−N[a]	0.11	0.29		0.21
Li−B				
$E_{HOMO-LUMO}$ (eV)	5.7	6.1	6.2	5.9

[a]M = Li, Al, Mg, and Ca.

In the calculations, the interactions of the Li and B atom show strong ionic characteristics in all four compounds. It is the reason that there is no contamination by BH_3 during the decomposition of bimetallic AMBs. Apparently, the relationship between Mg and N atom is of completely ionic nature. Among the other three, there are more or less covalent characters between metal atoms and N atoms where the Al−N bond exhibited the strongest one (0.29) while the Li−N bond (0.11) exhibited the weakest one, which is consistent with the DOS analysis. It should be mentioned that the radius of aluminum cation is the shortest in the four metals (R_{Li}^+ = 76 pm, R_{Mg}^{2+} = 72 pm, R_{Ca}^{2+} = 100 pm, R_{Al}^{3+} = 54 pm), so besides the obvious covalent characters between Al and N, the main relationship is still dominated by the electrostatic attraction. The populations of B−H and N−H indicate that they are both very stable covalent bonds. Generally, among the bimetallic AMBs, the results suggest that the bond strength of B−H bonds is stronger than that of the N−H bonds, which contradicts the findings of a previous study on metal aminoborane and monometallic ammine borohydrides.[42,43] So N−H bonds will be broken before B−H bonds in the decomposition. The HOMO−LUMO energy gap shows the sequence of stability of the four compounds: AMLB > AALB > ACLB > ALLB.

3.4. Decomposition Thermodynamics. In addition to the qualitative analyses on the physical and electronic structures, we further worked on the quantitative investigations of the dehydrogenation, deammoniation, and removal of borane by calculating the removal energy in each situation. All of the energies were calculated on the basis of the equation as AMB → [AMB − X] + X, where X means hydrogen, ammonia, and borane, respectively. After optimizing the 2 × 2 × 1 supercells of the four compounds, we remove one molecule of hydrogen (H(B) and H(N)), one NH_3 group, and one BH_3 group, respectively. For eliminating the interaction between the molecules, we built a cubic box (10 × 10 × 10 Å) for the molecules of H_2, NH_3, and BH_3, respectively. All of the

dx.doi.org/10.1021/jp5012439 | J. Phys. Chem. C 2014, 118, 8271−8279

structures including AMB, [AMB − X], and X have been calculated by CASTEP code.

During dehydrogenation, the strength of the host−guest hydrogen bonds can be quantified by the change in cohesive energy before and after the dissociation of hydrogen atom from the system.[44,45] From the analysis of the population, the H−N bond will be broken first. During this step, we removed hydrogen atoms from the weakest H−N bond and H−B bond to form a dihydrogen bond. The energy difference in the hydrogen-atom removal process is specified as ΔE_H. In the formula,[42,44] $E_{total}(AMB - H_2)$ denotes the Kohn−Sham energy of the AMB molecule after it has lost a molecular hydrogen, and $E_{total}(AMB)$ denotes the total electronic energy of primary AMB.

$$\Delta E_H = E_{total}(AMB - H_2) + E_{total}(H_2) - E_{total}(AMB)$$

As the experimental research, ALLB will release ammonia around 40 °C,[29] and more or less ammonia will be generated from AALB (less than 1% below 120 °C) and AMLB (1.1 wt % by 500 °C) in their decomposition. Moreover, the impurity product of borane was once a serious problem in the decomposition process. Considering the contamination of the reaction products, we also calculated the ammonia removal energy ($E_{total}(AMB - NH_3)$) and borane removal energy ($E_{total}(AMB - BH_3)$). We define their removal energies as ΔE_{NH_3} and ΔE_{BH_3} with the similar principle of hydrogen removal energy. The respective calculated removal energies are listed in Table 3.

$$\Delta E_{NH_3} = E_{total}(AMB - NH_3) + E_{total}(NH_3) - E_{total}(AMB)$$

$$\Delta E_{BH_3} = E_{total}(AMB - BH_3) + E_{total}(BH_3) - E_{total}(AMB)$$

Table 3. Removal Energy and Enthalpy (kcal/mol) of Hydrogen, Ammonia, and Borane at the Temperature of 298.15 K

reaction	ΔE	ΔH	reaction	ΔE	ΔH
ALLB − H_2	21.3	21.4	AMLB − H_2	−29.1	−29.0
ALLB − NH_3	17.8	17.7	AMLB − NH_3	26.6	26.8
ALLB − BH_3	64.1	64.0	AMLB − BH_3	9.1	9.0
AALB − H_2	3.4	3.4	ACLB − H_2	12.1	12.2
AALB − NH_3	27.9	27.8	ACLB − NH_3	16.6	16.7
AALB − BH_3	59.3	59.2	ACLB − BH_3	61.9	62.0

By comparing the hydrogen removal energies of the four compounds, we found that removing a molecule H_2 from ALLB required the most energy (21.3 kcal/mol). However, releasing ammonia from ALLB required lower energy (17.8 kcal/mol) than releasing hydrogen (21.3 kcal/mol), which suggests that ALLB more easily releases ammonia rather than hydrogen in the decomposition. The results are in agreement with the experiments showing that ammonia is almost the main product during the dissociation of ALLB. Additionally, $LiBH_4$ has been proved to have the potential to act as a highly effective ammonia store.[29] For ACLB, although the ammonia removal energy (16.6 kcal/mol) is the lowest in the four title compounds, it still prefers starting to dehydrogenate because of the lower initial hydrogen removal energy (12.1 kcal/mol).

Nevertheless, the hydrogen removal process of AMLB is an exothermic reaction with ΔE = −29.08 kcal/mol, which indicates a more stable reaction product as compared to those of AALB (ΔE = 3.4 kcal/mol) and ACLB (ΔE = 12.1 kcal/mol). Because the reaction free energy of dehydrogenation in AMLB ($\Delta G = \Delta H - T\Delta S(H_2)$) should be the lowest in the four compounds, we can confirm that the dehydrogenation of AMLB is the most favorable in the four compounds. Furthermore, the dehydrogenation energy of AALB is the second lowest in the four compounds, so it will also prefer to release hydrogen when starting decomposition. The low enthalpies for AMLB and AALB to dehydrogenate show the trend of the reactions.

From these results, we can not obtain the rates of dehydrogenation of different compounds. Yet from the experimental results, in which the dehydrogenation temperature of AMLB (begins at 95 °C) is higher than that of AALB (begins at 75 °C),[27,28] the barrier for AMLB releasing hydrogen should be higher than that for AALB, which is also consistent with the analysis of HOMO−LUMO energy gaps that AMLB is more stable than AALB. Actually, comparing the structures between ALLB and the other three AMBs, [$LiBH_4$] groups of M−Li ammine borohydrides (M = Mg, Al, Ca) have polarized the molecules and split the molecules into two ionic sections as [$LiBH_4$] and [M−NH_3]. The polarization will further activate the B−H···H−N bonds and decrease the hydrogen removal energies.

The deammoniation energies, with the exception of ALLB, are generally midway between the energies to remove hydrogen and borane. AALB requires the highest energy (27.9 kcal/mol) to remove ammonia, and it is slightly higher than that of AMLB, which indicates AMLB will emit ammonia easier than AALB and the weaker M−N bond strength of AMLB than AALB. The ammonia removal energies are consistent with the experiments where the hydrogen purities in the products of AMLB and AALB are 98.9% and more than 99%, respectively.[27,28] ACLB, as said before, shows even lower deammoniation energy than ALLB. The reason is possibly because of the radius of calcium (100 pm), which is bigger than that of lithium cation (76 pm), as well as a larger coordination number of calcium cation than lithium cation. So the bond strength between Ca and N is weaker than that of Li and N atoms. Caused by the polarization of two different metal cations, ACLB will start to dehydrogenate rather than deammoniate.

Commonly, releasing borane in the four compounds requires quite high energy due to the strong ionic interaction between the Li and BH_4 groups. Because it is difficult to break the bond of B−H(Li) to form BH_3 in AMBs mixed with $LiBH_4$, the contamination of borane will be effectively prevented and undetectable during the decomposition.

Table 3 summarizes the enthalpies of these reactants at 298.15 K. All of the Gibbs free energies (based on the equation of $\Delta G = \Delta E - T\Delta S(X)$, X means H_2, NH_3, and BH_3) have the same tendency of the reaction enthalpies, which all suggest the possible irreversibility of these decomposition reactions, too low or too high for near-ambient reversible storage. As well, we can obtain the decomposition trends of each reaction. From the results, the first step of AMLB will be more favorable to lose hydrogen under the moderate temperature, and next to that are AALB and ACLB. The last one is ALLB. Also, it seems impossible for the compounds to release ammonia (except for

dx.doi.org/10.1021/jp5012439 | J. Phys. Chem. C 2014, 118, 8271−8279

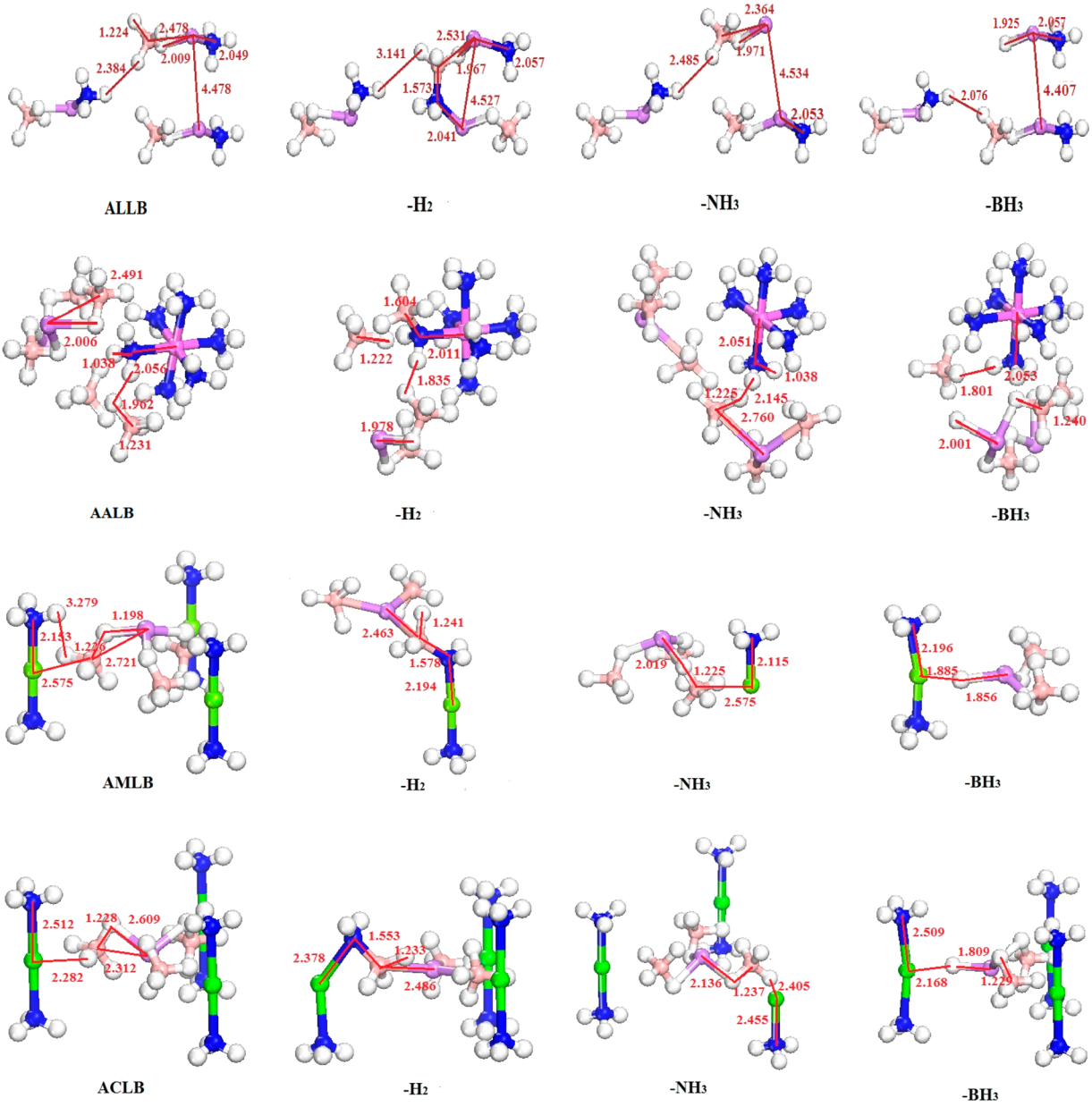

Figure 3. Local atomic structures of ALLB, AALB, AMLB, and ACLB before (the first column) and after the removal of the hydrogen (the second column), ammonia (the third column), and borane (the fourth column). Distances of the relative bonds are indicated with units in angstroms.

ALLB) and borane (especially for losing borane) at the start of their decomposition.

Figure 3 displays the structures from the supercells before and after the dehydrogenation, deammoniation, and removal of borane, which will shed light on the different initial decomposition process. For ALLB, the removal of hydrogen atoms leads to a significant rearrangement of the surrounding molecules. A $[Li(NH_2)(BH_4)]^-$ molecule almost turns over to form a new $[NH_2BH_3]$ like structure with its neighbored $[Li(NH_3)(BH_3)]^+$. The new N−B bond bridges the two molecules as a dimer structure. The new intermolecular B−N bond length is 1.573 Å, which is close to that bond length in $LiNH_2BH_3$ (1.571 Å).[46] At the same time, the distance of Li−Li has increased from 4.478 to 4.527 Å. After deammoniation, we noticed there is an ionic salt between $LiBH_4$ and $Li(NH_3)(BH_4)$. The bond length of Li−B is shortened from 2.478 to 2.364 Å. The distance of the Li−Li bond between two neighbored $Li(NH_3)(BH_4)$ structures increases from 4.478 to 4.534 Å, which may suggest the electronic repulsive force between the neighbored molecule has been increased after removal of ammonia. The distance between Li and N turns longer, which indicates the next ammonia molecular could be easier to release than the first one. Indeed, $LiBH_4$ as an excellent candidate for storing ammonia[29] implies $LiBH_4$ itself can absorb and emit ammonia very easily. In addition, after the removal of borane, all of the groups have been closed to each other. The distances between Li and N improved and the $[NH_3]$ group here acts like a ligand of LiH.

It is interesting to discover that a $[NH_2BH_3]$-like structure is formed after the dehydrogenation for the other three bimatallic AMBs similar to ALLB. The bond lengths of intermolecular B−N in AALB, AMLB, and ACLB after dehydrogenation are 1.604, 1.578, and 1.539 Å. After this structure is formed, the process may proceed similar to the decomposition of a

dx.doi.org/10.1021/jp5012439 | J. Phys. Chem. C 2014, 118, 8271−8279

bimetallic aminoborane.[47] Possibly, there will be another pathway in that the second dehydrogen can be formed on the basis of the electrostatic attraction between the $NH_2BH_2-H^{\delta-}$ and $NH_2-H^{\delta+}$ groups. Also, this should be furtherly confirmed by the energy barrier of kinetic study. In AALB, the distance of Li and B becomes longer and Al−N has been shortened after dehydrogenation, and that probably means a structure similar to the mixed metal amidoborane of Li−BH_3NH_2−Al has been formed as mentioned above. In AMLB and ACLB, the structures after dehydrogenation changed significantly when compared to the original structures. For instance, the NH_2 group in [AMLB − H_2] changes conformation to form the N−B dative bond, which elongates the bond length of Mg−N (from 2.153 to 2.194 Å). The distance of neighboring H(N)−H(B) bonds shortens apparently in AALB, AMLB, and ACLB, which specifies the interaction between $H^{\delta+}\cdots H^{\delta-}$ has been enhanced and the further energy barrier of dehydrogenation will be deduced. Interestingly, it seems that forming the structure of amidoborane after removal of hydrogenation shows excellent dehydrogenation properties from the results above except for ALLB because it is a monometallic AMB and also a great ammonia storage material. Therefore, it is a reasonable prediction because bimetallic amidoborane itself will suppress the emission of contamination.[31]

What is more with ALLB, it is intriguing to find that it will shorten the bond lengths of M−N (M denotes Mg, Al, and Ca) and accelerate the interaction of the metal cations and other NH_3 groups when we remove the ammonia from the original molecule in the other three compounds (Figure 3). As compared to ALLB, this also suggests that there are strong interactions between metals (Mg, Al, and Ca) and ammonia, and ammonia will not be released from the three compounds. The very large removal energies of deammoniation of AALB, AMLB, and ACLB also indicate it is hard to release ammonia at the beginning of decomposition. The truth is that almost no contamination of ammonia can be detected in the products in AALB and AMLB. Also, the limited contamination was predicted to be released from the structure of NH_2BH_3 after dehydrogenation with the increased temperature. As well, it is sensible to predict ACLB is a potential bimetallic AMB with excellent hydrogen-storage properties.

Although it seems impossible to remove the borane from the original structure for the high energy value, we also consider the decomposition of [BH_4] groups because the contamination of borane was once a serious problem of amidoborane,[48] and it will be helpful for us to look into the structure after removing the borane group. Except for ALLB, it is quite similar for the other three compounds, as the strong positive ionic interaction of metal cation leads to the phenomenon that the residual hydrogen atom will bridge the Mg/Al/Ca cations and Li^+. The intermolecular bond lengths of M−H further shorten, and structures of M−H−Li are formed (M means Mg, Al, and Ca), which suggests a more intense interaction between metals (Mg/Al/Ca) and other connected borane groups. For example, in ACLB, the bond length of intramolecular Li−B is reduced to 1.809 Å, while the intermolecular bond length of Ca−H is shortened to 2.168 Å. As an exception, there is only one valence charge for lithium cation, so it is favorable to form the more possible structure of LiH rather than to form a structure of Li−H−Li. After all, it is nearly impossible to release the borane in the bimetallic ammine borohydrides. These results further explain why deammoniation and removal of borane will hardly occur at the beginning because of the high removal energies and corresponding unstable product structures. Recently, some dehydrogenation mechanisms of AMBs have been elucidated for the NH_2-BH_3 complex in the process of decomposition.[10,29,44]

4. CONCLUSION

In this study, first-principles calculations were carried out on the solid M−Li ammine borohydrides (M = Li, Al, Mg, Ca). Although they have different geometries and chemical compositions, these materials have shown some common features. For instance, Li^+ cations stabilized the BH_4 groups and suppressed the impurity product of borane during the dissociation, and only the bimetallic AMBs show excellent hydrogen storage characters. A detailed study of the electronic structure revealed the highly ionic character of Mg cations in AMLB, whereas a more or less covalent bond character of Ca−N, Al−N, and Li−N was found in ACLB, AALB, and ALLB, respectively. On the basis of the HOMO−LUMO energy gap, we confirmed the order of stability of the four compounds to be as follows: AMLB > AALB > ACLB > ALLB. The thermodynamic study establishes that all of the decompositions are irreversible at room temperature. The three bimetallic AMBs have a preference to dehydrogenate rather than deammoniate at the beginning, while it is just the opposite situation in the decomposition process in ALLB. The first step of AMLB will be more favorable to loss of hydrogen under the moderate temperature; next to that are AALB and ACLB. Structural and energetic research reflects the formation of intermolecular dative N−B bonds when releasing hydrogen, whereas we propose it is more likely that $LiBH_4$ will promote the combination of B−N bonds in the dehydrogenation process in the bimetallic AMBs, which may lead to the excellent properties of dehydrogenation. Also, the impurities of ammonia and borane will be suppressed initially in the decomposition because of the effects of two different metals, and the large ΔE value to remove ammonia and borane initially. Except for ALLB, for itself it is an excellent material for storing ammonia. Finally, utilizing different metals is advantageous in changing the dehydrogenation properties of AMBs. We believe that our findings on bimetallic ammine borohydrides including the [$LiBH_4$] group are an important step in the ongoing development of AMBs as hydrogen storage materials.

AUTHOR INFORMATION

Corresponding Author

*Tel./fax: +86 10-68918091. E-mail: zjgbit@bit.edu.cn.

Notes

The authors declare no competing financial interest.

ACKNOWLEDGMENTS

We are thankful for financial support from the National Natural Science Foundation of China (NSFC 21071019), and the Program for New Century Excellent Talents in university (NCET-09- 0051). We are also thankful for the help of Prof. John E. McGrady, Dr. Vaida Arcisauskaite, and Dr. Dihao Zeng (Department of Chemistry, Inorganic Chemistry Laboratory, University of Oxford, South Parks Road, Oxford, OX1 3QR, UK).

REFERENCES

(1) Grochala, W.; Edwards, P. P. Thermal Decomposition of the Non-Interstitial Hydrides for the Storage and Production of Hydrogen. *Chem. Rev.* **2004**, *104*, 1283−1315.

(2) Kruger, P. Electric Power Requirement in the United States for Large-Scale Production of Hydrogen Fuel. *Int. J. Hydrogen Energy* **2000**, *25*, 1023−1033.

(3) Shevlin, S. A.; Guo, Z. X. Density Functional Theory Simulations of Complex Hydride and Carbon-based Hydrogen Storage Materials. *Chem. Soc. Rev.* **2009**, *38*, 211−225.

(4) U.S. Department of Energy. Development and Demonstration Plan: Planned Program Activities for 2005−2015, Technical Plan, U.S., 2005.

(5) Sakintuna, B.; Darkrim, L. E.; Hirscher, M. Requirements for Advanced Mobile Storage Systems. *Int. J. Hydrogen Energy* **2007**, *32*, 1121−1140.

(6) Brown, L. F. A Comparative Study of Fuels For On-board Hydrogen Production for Fuel-cell-powered Automobiles. *Int. J. Hydrogen Energy* **2001**, *26*, 381−397.

(7) Lipman, T. E.; Delucchi, M. A. Hydrogen-fuelled Vehicles. *Int. J. Veh. Des.* **1996**, *17*, 562.

(8) Fleischmann, M. Electrochemically Induced Nuclear Fusion of Deuterium. *J. Electroanal. Chem.* **1989**, *261*, 301−308.

(9) Soloveichik, G.; Her, J. H.; Stephens, P. W.; Gao, Y.; Rijssenbeek, J.; Andrus, M.; Zhao, J. C. Ammine Magnesium Borohydride Complex as a New Material for Hydrogen Storage: Structure and Properties of $Mg(BH_4)_2{\cdot}2NH_3$. *Inorg.Chem.* **2008**, *47*, 4290−4298.

(10) Gu, Q. F.; Gao, L.; Guo, Y. H.; Tan, Y. B.; W.Tang, Z.; Wallwork, K. S.; Zhang, F. W.; Yu, X. B. Structure and Decomposition of Zinc Borohydride Ammonia Adduct: Towards a Pure Hydrogen Release. *Energy Environ. Sci.* **2012**, *5*, 7590−7600.

(11) Brown, G. M.; Knight, D. A.; Rawn, C. J.; Santos, A. F.; Schneibel, J. H.; Sloop, F. V. Preparation and Reactions of Complex Hydrides for Hydrogen Storage: Metal Borohydrides and Aluminum Hydrides. *Hydrogen Storage* **2009**, 467−471.

(12) Yuan, F.; Gu, Q. F.; Guo, Y. H.; Sun, W. W.; Chen, X. W.; Yu, X. B. Structure and Hydrogen Storage Properties of the First rare-earth Metal Borohydride Ammoniate: $Y(BH_4)_3.4NH_3$. *J. Mater. Chem.* **2012**, *22*, 1061−1068.

(13) Yuan, F.; Gu, Q. F.; Chen, X. W.; Tan, Y. B.; Guo, Y. H.; Yu, X. B. Complex Ammine Titanium(III) Borohydrides as Advanced Solid Hydrogen-Storage Materials with Favorable Dehydrogenation Properties. *Chem. Mater.* **2012**, *24*, 3370−3379.

(14) Wang, K.; Zhang, J. G.; Man, T.-T.; Wu, M.; Chen, C. C. Recent Process and Development of Metal Aminoborane. *Chem. Asian J.* **2013**, *8*, 1076 −1089.

(15) Chu, H. L.; Wu, G. T.; Xiong, Z. T.; Guo, J. P.; He, T.; Chen, P. Structure and Hydrogen Storage Properties of Calcium Borohydride Diammoniate. *Chem. Mater.* **2010**, *22*, 6021−6028.

(16) Guo, Y. H.; Jiang, Y. X.; Xia, G. L.; Yu, X. B. Ammine Aluminium Borohydrides: An Appealing System Releasing Over 12 wt % Pure H_2 Under Moderate Temperature. *Chem. Commun.* **2012**, *48*, 4408−4410.

(17) Xia, G. L.; Tan, Y. B.; Chen, X. W.; Guo, Z. P.; Liu, H. K.; Yu, X. B. Mixed-metal (Li, Al) Amidoborane: Synthesis and Enhanced Hydrogen Storage Properties. *J. Mater. Chem. A* **2013**, *1*, 1810−1820.

(18) Pinkerton, F. E.; Meyer, M. S.; Meisner, G. P.; Balogh, M. P.; Vajo, J. J. Phase Boundaries and Reversibility of LiBH4/MgH2 Hydrogen Storage Material. *J. Phys. Chem. C* **2007**, *111*, 12881−12885.

(19) Chen, X. W.; Yuan, F.; Tan, Y. B.; Tang, Z. W.; Yu, X. B. Improved Dehydrogenation Properties of $Ca(BH_4)_2{\cdot}nNH_3$ (n = 1, 2, and 4) Combined with $Mg(BH_4)_2$. *J. Phys. Chem. C* **2012**, *116*, 21162−21168.

(20) Richardson, B. S.; Birdwell, J. F.; Pin, F. G.; Jansen, J. F.; Lind, R. F. Sodium Borohydride Based Hybrid Power System. *J. Power Sources* **2005**, *145*, 21−29.

(21) Kim, D. Y.; Lee, H. M.; Seo, J.; Shin, S. K.; Kim, K. S. Rules and Trends of Metal Cation Driven Hydride-transfer Mechanisms in Metal Amidoboranes. *Phys. Chem. Chem. Phys.* **2010**, *12*, 5446−5453.

(22) Luedtke, T. A.; Autrey, T. Hydrogen Release Studies of Alkali Metal Amidoboranes. *Inorg. Chem.* **2010**, *49*, 3905−3910.

(23) Kang, X. D.; Luo, J. H.; Wang, P. Efficient and Highly Rapid Hydrogen Release from Ball-milled $3NH_3BH_3/MMgH_3$ (M = Na, K, Rb) Mixtures at Low Temperatures. *Int. J. Hydrogen Energy* **2012**, *37*, 4259−4266.

(24) Ravnsbæk, D.; Filinchuk, Y.; Cerenius, Y.; Jakobsen, H. J.; Besenbacher, F.; Skibsted, J.; Jensen, T. R. A Series of Mixed-Metal Borohydrides. *Angew. Chem., Int. Ed.* **2009**, *48*, 6659 −6663.

(25) Tang, Z. W.; Tan, Y. B.; Gu, Q. F.; Yu, X. B. A Novel Aided-cation Strategy to Advance the Dehydrogenation of Calcium Borohydride Monoammoniate. *J. Mater. Chem.* **2012**, *22*, 5312−5318.

(26) Liu, B.; Chua, Y. S.; Wu, G. T.; Xiong, Z. T.; Chen, P. Synthesis and Dehydrogenation of LiCa(NH2)3(BH3)2. *Int. J. Hydrogen Energy* **2012**, *37*, 9076−9081.

(27) Sun, W. W.; Chen, X. W.; Gu, Q. F.; Wallwork, K. S.; Tan, Y. B.; Tang, Z. W.; Yu, X. B. A New Ammine Dual-Cation (Li, Mg) Borohydride: Synthesis, Structure, and Dehydrogenation Enhancement. *Chem.—Eur. J.* **2012**, *18*, 6825−6834.

(28) Guo, Y. H.; Wu, H.; Zhou, W.; Yu, X. Dehydrogenation Tuning of Ammine Borohydrides Using Double-Metal Cations. *J. Am. Chem. Soc.* **2011**, *133*, 4690−4693.

(29) Guo, Y.; Xia, G.; Zhu, Y.; Gao, L.; Yu, X. Hydrogen Release from Ammine Lithium Borohydride, $LiBH_4NH_3$. *Chem. Commun.* **2010**, *46*, 2599−2601.

(30) Diyabalanage, H. V. K.; Nakagawa, T.; Shrestha, R. P.; Semelsberger, T. A.; Davis, B. L.; Scott, B. L.; Burrell, A. K.; David, W. I. F.; Ryan, K. R.; Jones, M. O.; Edwards, P. P. Potassium(I) Amidotrihydroborate: Structure and Hydrogen Release. *J. Am. Chem. Soc.* **2010**, *132*, 11836−11837.

(31) Xiong, Z. T.; Yong, C. K.; Wu, G. T.; Chen, P.; Shaw, W.; Karkamkar, A.; Autrey, T.; Jones, M. O.; Johnson, S. R.; Edwards, P. P.; David, W. I. F. High-capacity Hydrogen Storage in Lithium and Sodium Amidoboranes. *Nat. Mater.* **2008**, *7*, 138−141.

(32) Zhang, Y. S.; Wolverton, C. Crystal Structures, Phase Stabilities, and Hydrogen Storage Properties of Metal Amidoboranes. *J. Phys. Chem. C* **2012**, *116*, 14224−14231.

(33) Blochl, P. E. Projector Augmented-wave Method. *Phys. Rev. B* **1994**, *50*, 17953−17979.

(34) Segall, M. D.; Lindan, P. J. D.; Probert, M. J.; Pickard, C. J.; Hasnip, P. J.; Clark, S. J.; Payne, M. C. First-principles Simulation: Ideas, Illustrations and the CASTEP Code. *J. Phys.: Condens. Matter* **2002**, *14*, 2717.

(35) Perdew, J. P.; Wang, Y. Accurate and Simple Analytic Representation of The Electron-gas Correlation Energy. *Phys. Rev. B* **1992**, *45*, 13244−3249.

(36) Perdew, J. P.; Burke, K.; Ernzerhof, M. Generalized Gradient Approximation Made Simple. *Phys. Rev. Lett.* **1996**, *77*, 3865−3868.

(37) Vanderbilt, D. Soft Self-consistent Pseudopotentials in a Generalized Eigenvalue Formalism. *Phys. Rev. B* **1990**, *41*, 7892−7895.

(38) Monkhorst, H. J.; Pack, J. D. Special points for Brillouin-zone Integrations. *Phys. Rev. B* **1976**, *13*, 5188−5192.

(39) Fischer, T. H.; Almlof, J. General Methods for Geometry and Wave Function Optimization. *J. Phys. Chem.* **1992**, *96*, 9768−9774.

(40) Delley, B. From Molecules to Solids with the $DMol^3$ Approach. *J. Chem. Phys.* **2000**, *113*, 7756−7764.

(41) Godby, R. W.; Schlüter, M. Accurate Exchange-Correlation Potential for Silicon and Its Discontinuity on Addition of an Electron. *Phys. Rev. Lett.* **1986**, *56*, 2415−2418.

(42) Li, W.; Scheicher, R. H.; Araujo, C. M.; Wu, G. T.; Blomqvist, A.; Wu, C. Z.; Ahuja, R.; Feng, Y. P.; Chen, P. Understanding from First-Principles Why $LiNH_2BH_3.NH_3BH_3$ Shows Improved Dehydrogenation over $LiNH_2BH_3$ and NH_3BH_3. *J. Phys. Chem. C* **2010**, *114*, 19089−19095.

(43) Ramzan, M.; Silvearv, F.; Blomqvist, A.; Scheicher, R. H.; Lebegue, S.; Ahuja, R. Structural and Energetic Analysis of The Hydrogen Storage Materials $LiNH_2BH_3$ and $NaNH_2BH_3$ from Ab Initio Calculations. *Phys. Rev. B* **2009**, *79*, 1−3.

(44) Chen, X. W.; Yu, X. B. Electronic Structure and Initial Dehydrogenation Mechanism of $M(BH_4)_2{\cdot}2NH_3$ (M = Mg, Ca, and Zn): A First-Principles Investigation. *J. Phys. Chem. C* **2012**, *116*, 11900−11906.
(45) Siegel, D. J.; Wolverton, C. Reaction Energetics and Crystal Structure of Li4BN3H10 from First Principles. *Phys. Rev. B* **2007**, *75*, 014101−014112.
(46) Lee, S. M.; Kang, X. D.; Wang, P.; Cheng, H. M.; Lee, Y. H. A Comparative Study of the Structural, Electronic, and Vibrational Properties of NH_3BH_3 and $LiNH_2BH_3$: Theory and Experiment. *ChemPhysChem* **2009**, *10*, 1825−1833.
(47) Fijalkowski, K. J.; Jurczakowski, R.; Wiktor, K.; Wojciech, G. Insights from Impedance Spectroscopy into the Mechanism of Thermal Decomposition of $M(NH_2BH_3)$, M = H, Li, Na, $Li_{0.5}Na_{0.5}$, Hydrogen Stores. *Phys. Chem. Chem. Phys.* **2012**, *14*, 5778−5784.
(48) Lane, C. F. *Ammonia-Borane and Related N-B-H Compounds and Materials: Safety Aspects, Properties and Applications*; Northern Arizona University, 2006; pp 1−33.